A tissue-scale gradient of hydrogen peroxide mediates rapid wound detection in zebrafish

Philipp Niethammer[1,*], **Clemens Grabher**[2,3,*], **A. Thomas Look**[2,4], and **Timothy J. Mitchison**[1]

[1]Departement of Systems Biology, Harvard Medical School, Boston MA 02115, USA

[2]Department of Pediatric Oncology, Dana-Farber Cancer Institute, Harvard Medical School, Boston, MA 02115, USA

[4]Division of Hematology/Oncology, Department of Pediatrics, Children's Hospital, Harvard Medical School, Boston, MA 02114, USA

Abstract

Barrier structures (e.g. epithelia around tissues, plasma membranes around cells) are required for internal homeostasis and protection from pathogens. Wound detection and healing represent a dormant morphogenetic program that can be rapidly executed to restore barrier integrity and tissue homeostasis. In animals, initial steps include recruitment of leukocytes to the site of injury across distances of hundreds of micrometers within minutes of wounding. The spatial signals that direct this immediate tissue response are unknown.

Due to their fast diffusion and versatile biological activities, reactive oxygen species (ROS), including hydrogen peroxide (H_2O_2), are interesting candidates for wound-to-leukocyte signalling. We probed the role of H_2O_2 during the early events of wound responses in zebrafish larvae expressing a genetically encoded H_2O_2 sensor1. This reporter revealed a sustained rise in H_2O_2 concentration at the wound margin, starting ∼3 min after wounding and peaking at ∼20 min, which extended ∼100–200 μm into the tail fin epithelium as a decreasing concentration gradient. Using pharmacological and genetic inhibition, we show that this gradient is created by Dual oxidase (Duox), and that it is required for rapid recruitment of leukocytes to the wound. This is the first observation of a tissue-scale H_2O_2 pattern, and the first evidence that H_2O_2 signals to leukocytes in tissues, in addition to its known antiseptic role.

Hydrogen peroxide (H_2O_2) is a chemically relatively stable ROS that can diffuse in tissues and cross cell membranes2, making it an interesting candidate for paracrine tissue signalling. Plants exploit H_2O_2 as a paracrine signal to regulate xylem differentiation and

[3]Current address: Karlsruhe Institute of Technology, Forschungszentrum Karlsruhe GmbH, 76344 Eggenstein-Leopoldshafen, Germany
[*]These authors contributed equally to this work

Supplementary Information is linked to the online version of the paper at www.nature.com/nature.

lignification2. Known signalling roles of H_2O_2 in animals are primarily within the cytoplasm, where it regulates metabolism, phosphatase activity and gene transcription, and causes oxidative damage at higher concentrations3. Paracrine signalling has been seen in cell culture experiments, but these may not faithfully mimic extracellular conditions in tissues2.

To investigate possible paracrine signalling by H_2O_2, we imaged its spatiotemporal dynamics, together with leukocyte motility, in an intact vertebrate tissue subjected to mechanical wounding. The zebrafish larval tail fin has become a popular vertebrate model system to study inflammatory and regenerative responses to wounds4-7. Rapid leukocyte recruitment to the wound can be easily imaged, and the molecular dynamics of the tissue perturbed using morpholino knockdown, transgenic expression and pharmacology.

We measured H_2O_2 by expressing HyPer, a genetically encoded ratiometric sensor that is highly selective for H_2O_2 over other ROS1. HyPer consists of the bacterial H_2O_2-sensitive transcription factor OxyR fused to a circularly permuted YFP. Cysteine oxidation of the OxyR part induces a conformational change that increases emission excited at 500 nm (YFP_{500}) and decreases emission excited at 420 nm (YFP_{420}). This change is rapidly reversible within the reducing cytoplasmic environment, allowing dynamic monitoring of intracellular H_2O_2 concentration. We introduced HyPer by mRNA injection into zebrafish embryos to induce global cytoplasmic expression (Figure 1a) and confirmed that HyPer ratios respond to externally added H_2O_2 (Supplementary Figure S1a).

Upon local injury of the tail fin of zebrafish larvae at 3 days post fertilization (3 dpf), we observed a rapid and dramatic increase in HyPer ratio signal (YFP_{500}/YFP_{420}) at the wound margin (Figure 1b, Supplementary Movie 1). To test if this was caused by an unspecific environmental effect (e.g. pH change), we expressed YFP alone, and observed only a marginal fluorescence increase, most likely due to ruffling/contraction of the wound margin inducing a local increase in tissue thickness (Supplementary Figure S1b). Similarly, the pH reporter BCECF-AM did not indicate a major contribution of pH to the wound margin signal. H_2O_2 production at the wound margin was confirmed by using the H_2O_2 selective fluorogenic probe acetyl-pentafluorobenzenesulfonyl fluorescein8 (Supplementary Figure S1c). Hence, the primary wound margin signal is due to H_2O_2 or a closely related molecule; HyPer does not respond to superoxide (O_2^-) or nitric oxide (NO)1. The H_2O_2 signal peaked $\sim$20 min post wounding (pw) (Figure 1c). At this time, the observable H_2O_2 gradient extended $\sim$100–200 μm inward from the wound margin (Figure 1d), so its low concentration end approached the nearest blood vessel.

We quantified leukocyte recruitment to the wound by imaging transmitted light and two different leukocyte-specific fluorescent tags, *mpo::GFP*9 (Figure 2d, 3c) and *lysC::DsRED2*10 (Figure 1e). Some leukocytes were patrolling the fin at the time of wounding, while others were apparently recruited from the vasculature. Excluding occasional cases where a leukocyte was already present at the wound site, the first leukocyte arrived at the wound margin 17 ± 6 min pw (mean ± SD of n=14 larvae). This timing is superimposed on a typical H_2O_2 profile in Figure 1c. Wound margin H_2O_2 production clearly preceded recruitment of the first leukocyte in most cases (see also Figure 1e,

Supplementary Figure S1d, Supplementary Movie 2), indicating that the source of H_2O_2 must be tail fin epithelial cells, not leukocytes. This finding runs counter to the prevailing view that ROS production during inflammatory responses originates from leukocyte oxidative bursts[11].

The main physiological source of extracellular H_2O_2 is likely to be NADPH oxidases (NOXes), which transport electrons from cytoplasmic NADPH to generate O_2^- or H_2O_2 in phagosomes or outside the cell[12]. The zebrafish genome encodes Nox1, Nox2 (leukocyte oxidase), Nox4, Nox5 and a single isoform of Duox[13] (Figure 2a). Nox1−5 generate superoxide, which can be dismutated into H_2O_2 by separate superoxide dismutase (SOD) enzymes, while Duox generates H_2O_2 without requiring a separate SOD[14]. To test for a role of any Nox enzyme in generating wound margin H_2O_2, we added two structurally unrelated small molecule inhibitors of the whole family, diphenyleneiodonium (DPI) and VAS2870[15-18] to the bathing water prior to wounding. Both efficiently inhibited H_2O_2 production without obvious toxicity (Figure 2b, c; Supplementary Movie 3).

We next quantified leukocyte recruitment in the *mpo::GFP* fish line[9] during the peak period of H_2O_2 production. Under control conditions, an average of 4−6 leukocytes arrived at the wound margins within the first 42 min pw. Nox inhibition strongly attenuated leukocyte recruitment to the wound during this initial phase of the response, with less than one leukocyte arriving, on average, in drug-treated larvae (Figure 2d, e; Supplementary Movie 4).

The specific Nox that generates wound margin H_2O_2 was identified by targeting pre-mRNA splice sites with antisense morpholinos. Interference with pre-mRNA splicing of P22phox (*cyba*), an essential subunit of Nox1−4[12], led to quantitative conversion of its mRNA level into a mutant with a premature stop-codon that likely terminated translation of P22phox after the 28th amino acid residue (Supplementary Figure S2c, inset). This had no effect on the H_2O_2 gradient (Supplementary Figure S2a, b, c; Supplementary Movie 5), or leukocyte recruitment to the wound (Supplementary Figure S2d). Nox5 and Duox remained as candidates. By semi-quantitative PCR we confirmed that *duox* but not *nox5* is expressed in tail fin tip tissue (Supplementary Figure S3c). In mammals, DUOX is mainly expressed in the thyroid gland, where it generates H_2O_2 for organification of I^-[19], but also in epithelial surfaces that contact liquid environments, including the luminal surface of the gut and lung. Extracellular H_2O_2 made by DUOX is thought to react with halide or thiocyanate, catalyzed by secreted lactoperoxidases (LPOs), to generate more reactive ROS species that kill luminal bacteria[20,21]. DUOX contains two Ca^{2+} binding EF-hand motives and, at least in cell culture, can be activated by Ca^{2+}-mobilizing small molecules[22], and by mechanical cell injury[23], making it a good candidate for wound signalling.

Morpholino-induced perturbation of *duox* pre-mRNA splicing (Figure 3b, inset) caused a developmental morphology phenotype characterized by cell death predominantly in the head region. This phenotype is probably specific for *duox* knockdown, since two independent splice morpholinos, but not a corresponding 5-misprime morpholino, induced the same phenotype (not shown). To generate morphologically normal tail fins for the assay, we co-knocked down *p53*, which partially rescued the *duox* knockdown morphological phenotype.

Strikingly, we found a significant reduction of wound induced H_2O_2 production in *duox/p53* knockdown larvae compared to *duox 5-MP/p53* controls (Figure 3a, b; Supplementary Figure S2a, Supplementary Movie 6). Further, *duox* knockdown strongly attenuated recruitment of leukocytes to the wound (Figure 3c, d; Supplementary Movies 7, 8). This attenuation was not caused by a reduction of total leukocyte number in *duox* knockdown embryos (Supplementary Figure S2e). *Duox* knockdown did cause a significant reduction in the number of leukocytes infiltrating the tail fin following wounding, reducing it to near the level seen in un-wounded fins (Supplementary Figure S3a). It also caused a significant decrease in directional migration towards the wound, while basal leukocyte motility, as observed in the absence of a wound, was not affected. These data implicate Duox as the main source of wound margin H_2O_2 required for rapid leukocyte recruitment.

In conclusion, we visualized for the first time a tissue-scale gradient of H_2O_2 induced by wounding, found that it is generated by Duox activity in epithelial cells, and showed that it is required for leukocyte recruitment to the wound. Based on published calibration of HyPer in tissue culture1, wound-induced extracellular H_2O_2 may reach concentrations of ∼0.5–50 μM near the wound margin. The gradient was established within 10 min of wounding, and gradually dissipated over ∼1–2 hrs. Visual inspection of movies (Figure 1e, 2d, 3c) suggested that leukocytes sensed the wound within ∼10 min, from distances as large as 200 μm. Thus, the spatiotemporal scales of the H_2O_2 gradient, and the leukocyte response, were roughly similar. Trajectory analysis showed that the H_2O_2 gradient stimulated leukocyte recruitment mainly by increasing directionality of leukocyte migration and tissue infiltration, (Supplementary Figure S3a, movies 4, 8). This argues against a permissive role of extracellular H_2O_2 for basal leukocyte motility in our assay, and favours the idea that wound margin H_2O_2 production spatially instructs rapid wound recruitment of leukocytes, either by direct chemotactic signalling, or by stimulating production of some downstream chemoattractant. Direct chemotactic activity of H_2O_2 was previously demonstrated *in vitro* for neutrophils24 and vascular smooth muscle cells25, at concentrations24 (∼10 μM) that are roughly consistent with our estimation of wound margin [H_2O_2]. Together with our data, this raises the striking possibility that H_2O_2 itself acts as a paracrine, chemotactic signal during the initial phase of wound detection. Leukocytes might express trans-membrane receptors for H_2O_2; none are known, but T-type Ca^{2+} channels are thought to have this function in sensory neurons26. Alternatively, H_2O_2 might direct migration by entering the cytoplasm and locally modifying intracellular receptors, such as the redox sensitive phosphatase PTEN27. PtdIns(3,4,5)P(3) phosphatases such as PTEN or SHIP-1 are thought to be important regulators of chemo- and electro-tactic responses28-30. Our current data do not distinguish whether the spatial H_2O_2 gradient reflects diffusion from a localized source at the wound margin combined with global breakdown by catalases and/or peroxidases, or rather a gradient of H_2O_2 production induced by some upstream regulatory pattern, such as an electric field or a spatial gradient of an upstream signalling molecule. DUOX was previously implicated in constitutive ROS-induced microbial killing by mucosal epithelia19. Our data implicate it, for the first time, as a major, non-myeloid ROS source in the initial phase of inflammation. We hypothesize that the DUOX/LPO system evolved to simultaneously play two useful roles in early responses to epithelial wounding, local killing

of potential invading bacteria, and rapid recruitment of phagocytic leukocytes from distant sites.

Methods Summary

Imaging of H_2O_2 and leukocytes in zebrafish

1-cell stage zebrafish embryos were injected with HyPer mRNA. 3 dpf larvae were subjected to tail fin tip amputation and mounted in 1% low-melting agarose. HyPer fluorescence was excited with 501/16 and 420/40 bandpass excitation filters and corresponding YFP emission was acquired every 2 min within 3–42 min after injury using a 535/30 bandpass emission filter. For calculating HyPer ratio images, smoothed, background subtracted and thresholded YFP_{500} and YFP_{420} images were divided.

Leukocytes were imaged every 30 sec within 3–42 min after tail fin incision of fluorescent leukocyte reporter zebrafish larvae. Leukocyte migration to the wound was observed both by fluorescence and transmission imaging. Final leukocyte count at the wound margin was assessed 42 min after injury.

Zebrafish larvae were anesthetized for wounding and imaging experiments. All buffers were sterile filtered. Blades were treated with 70% ethanol prior to use. Imaging was optimized for low illumination, and performed on an inverted widefield microscope equipped with a CCD camera and a mercury illumination source.

Genetic and pharmacological perturbations

Anesthetised larvae were incubated with pharmacological compounds up to 40 min prior to wounding and during imaging. Antisense morpholinos were injected into 1-cell stage embryos. Morpholino-mediated splice perturbation was confirmed by RT-PCR. Full Methods and any associated references are available in the online version of the paper at www.nature.com/nature.

Supplementary Material

Refer to Web version on PubMed Central for supplementary material.

Acknowledgements

Methods

General fish procedures

Zebrafish strains AB, *mpo::GFP*9, and *lysC::DsRED2*10 were maintained as described31. For wounding assays, zebrafish were anesthetized in E3 (5 mM NaCl, 0.17 mM KCl, 0.33 mM $CaCl_2$, 0.33 mM $MgSO_4$) containing 0.1 mg/ml Tricaine (Sigma) prior to wounding. To prevent pigment formation, larvae were maintained in E3 containing 0.2 mM N-

phenylthiourea (PTU; Sigma). All buffers were sterile filtered and blades were sterilized using 70% ethanol prior to use.

Imaging the wound response

For all imaging, larvae were maintained in E3 supplemented with 0.1 mg/ml Tricaine.

For imaging of H_2O_2 production, 1-cell stage zebrafish embryos were injected with HyPer1 mRNA (~ 0.5 mg/ml). 3 dpf larvae were subjected to tail fin tip amputation using a needle knife (Fine Science Tools) and embedded in 1% low melting agarose (Lonza) in a glass bottom dish (Matek Corporation). Every 2 min starting ~ 3 min pw, HyPer fluorescence was excited using 420/40 and 501/16 bandpass filters (Chroma), and YFP emission was acquired using a 535/30 bandpass filter.

For alternative H_2O_2 imaging, 2–3 dpf larvae were loaded ~ 60 min with 50 μM Acetyl-pentafluorobenzenesulfonyl fluorescein (Calbiochem) prior to wounding. Emission was excited using 484/15 bandpass filter (Chroma) and acquired using a 525/50 bandpass filter (Chroma).

For pH imaging, 2–3 dpf larvae were loaded ~ 60 min with 50 μM 3'-O-Acetyl-2',7'-bis(carboxyethyl)-4 or 5-carboxyfluorescein diacetoxymethyl ester (BCECF-AM, Calbiochem) prior to wounding. Emission was excited using 484/15 bandpass filter (Chroma) and acquired using a 535/30 bandpass filter (Chroma). For imaging of leukocyte recruitment, 3–5 dpf *mpo::GFP* or *lysC::DsRED2* larvae were cut at the tail fin using a tungsten needle (Fine Science Tools), mounted in agarose, and leukocyte fluorescence was excited using a 484/15 or 540/15 bandpass filter (Chroma). Emission was acquired every 30 sec using a 525/50 or 610/80 bandpass filter (Chroma). All images were acquired at room temperature ($\sim 26°C$) using Metamorph (Molecular Devices) and a Nikon Eclipse TE300 microscope equipped with 20x plan-apochromate NA 0.75 air objective lens, an ORCA-ER camera (Hamamatsu), and a mercury light source (Chiu Technical Corporation).

Tail fin tip amputation (needle blade) was used in all HyPer assays, tail fin incision (tungsten needle) in all chemotaxis assays. Only same types of cuts were directly compared. The HyPer signal was not dependent on the type of cut (Supplementary Figure S3b).

Generally, each imaging setup was optimized for minimal light exposure of larvae. Whenever possible, we used two neutral density filters (except for BCECF-AM were dye loading was rather inefficient, so that we had to use one neutral density filter), highest camera gain, and high binning (e.g. 8×bin for probe imaging, 4×bin for leukocyte imaging).

Image processing and data analysis

For calculating HyPer ratio images, smoothed (one-pass median filter), background subtracted and thresholded YFP_{500} and YFP_{420} images were divided (YFP_{500}/YFP_{420}) using ImageJ (NIH) or Matlab (Mathworks). Up-regulation of H_2O_2 was calculated by dividing the mean ratio acquired in a region of interest directly at the wound margin (rat_{wound}) by the mean basal ratio acquired in a region of interest inside the body (rat_{basal}, $\sim 300 - 400$ μm

distant from the wound margin). H_2O_2 up-regulation was expressed either as multiple ($f_{mult}=rat_{wound}/rat_{basal}$; e.g. Supplementary Figure 2b) or fraction of the base level ($f_{fract}= (rat_{wound}-rat_{basal})/rat_{basal}$). Relative H_2O_2 production at wound margin (e.g. Figure 2c, 3b) was derived as f_{fract} normalized to the control ($f_{rel}=f_{fract}(sample)/f_{fract}(control)$).

Leukocyte recruitment was determined by counting all migrating cells that arrived at the wound margin within 42 min pw as judged from the 30 sec/frame time-lapse movies of *mpo::GFP* leukocyte reporter fish (transmission and GFP channel). Cells that already resided at the wound margin at the beginning of the time-lapse sequence (∼3 min pw) were not counted.

Leukocyte trajectory analysis

Trajectory analysis was performed on the same leukocyte time-lapse data that was also used to quantify wound recruitment of leukocytes. Trajectories were generated by marking the approximate center of mass of those cells that moved in the ventral tail fin, and could be identified with adequate reliability. Only those cells were included in the statistical path analysis that described a path of at least 50 μm. Further, tracks or part of tracks within a radius of 50 μm around the center of mass of the triangular wound region were not included into the analysis in order to avoid tracking of cells that had already reached the wound, and merely moved along the wound margins. Average velocity (v_{av}) was calculated as $v_{av} = l_{track} / t_{track}$, with l_{track} being the length of the track, and t_{track} being the total track time.

Path linearity (which is frequently also termed "directionality") was calculated as $Dir_p = d_{OE} / l_{track}$, with d_{OE} being the Euclidian distance between origin (O) and endpoint (E) of the track.

Wound directionality was calculated as $Dir_w = (d_{OW}-d_{EW})/l_{track}$, with d_{OW} being the distance between track origin and center of mass of the wound (W), and d_{EW} being the distance between track endpoint and W.

Pharmacological and morpholino treatments

Larvae were incubated in E3 supplemented with 100 μM DPI (Sigma), 20 μM VAS2870, 1% DMSO (Sigma) 30–40 min prior to wounding. Mounting agarose and imaging medium (E3) were supplemented with the indicated compound concentrations.

The following splice morpholinos (Gene Tools) were injected into 1-cell stage larvae (∼ 0.5 – 1 mM):

MO-*cyba*: 5'- ATCATAGCATGTAAGGATACATCCC-3';

MO1-*duox*: 5'- AGTGAATTAGAGAAATGCACCTTTT-3';

MO5-MP-*duox* (5-MP): 5'- AGTcAATTAcAGAAATcCAgCTaTT-3';

MO2-*duox*: 5'- ACATTCACTCTCTCACCTGGATATG-3'.

For morphotyping, RNA was prepared from 3 dpf larvae by phenol-chloroform extraction (TRI solution, Ambion), and one-step RT-PCR (Qiagen) was performed to confirm knockdown efficiency using the following primers:

cyba fwd: 5'-GCGAAGATTGAGTGGGCGATGTGGGCC-3';

cyba rev: 5'-TTATTCGTTGATGGTGACAGACATAGGATTGTC-3';

duox fwd: 5'-ACACATGTGACTTCATATCCAG-3';

duox rev: 5'-ATTATTAACTCATCCACATCCAG-3'.

The RT-PCR products were sequenced. MO-*cyba* mediated splice perturbation produced a 146 bp deletion in the *cyba* mRNA, introducing a premature stop-codon into the resulting splice-mutant mRNA, coding for 28 AA truncated translation product. MO1-*duox* mediated splice perturbation produced a 39 bp in-frame deletion within the peroxidase-like domain of *duox*. MO1-*duox* and MO2-*duox* produced identical phenotypes; however, MO2-*duox* injected larvae yielded neither detectable wt-, nor splice-mutant amplification product, while *beta-actin* could successfully be amplified from the same template. This indicated that MO2-*duox* resulted in *duox* mRNA knockdown, either by generating a splice-mutant mRNA that was rapidly degraded, or too large to be amplified under our conditions. For phenotypical rescue of the tail fin in the HyPer and leukocyte migration assays, MO1-*duox*, and MO5-MP-*duox* (5-MP) morpholinos were generally co-injected with a morpholino inhibiting *p53* mRNA translation (~ 0.2 mM, 5'- GCGCCATTGCTTTGCAAGAATTG -3'32).

Cell sorting

Larvae (~150) were collected from Tg(*mpo::GFP*) at 80 hpf and disaggregated into a single cell suspension as previously described33. Sorting of *mpo::GFP* positive cells was performed on a BD Aria based on GFP fluorescence.

RNA isolation and semi-quantitative RT-PCR

Total RNA from amputated tailfins (80 hpf) or sorted GFP+ cells was extracted with TRIzol (Invitrogen). RT-PCR was performed with a one-Step RT-PCR Kit (Qiagen) according to the manufacturers protocol using 35 cycles on 2 ng total RNA with intron-spanning primers.

Oligo sequences were as follows:

duox fwd: 5'-GTTGGCTTTGGTGTAACTGTA-3';

duox rev: 5'-GCCCAGGCTGTGAGAG-3';

nox5 fwd: 5'-TGGCCTAATGGTGGTCTGTTC-3';

nox5 rev: 5'-CAGAGCCGAAACCCAGATG-3';

beta-actin fwd: 5'-CATTGGCAATGAGCGTTTC-3';

beta-actin rev: 5'-TACTCCTGCTTGCTGATCCAC-3'.

Statistics

All error bars indicate standard errors of means (SEM). All p-values have been derived by an unpaired, two-tailed t-test assuming unequal variances (heteroscedastic) using Excel (Microsoft).

References

31. Nusslein-Volhard, C.; Dahm, R. Zebrafish. Oxford University Press; NY: 2002.

32. Chen J, et al. Loss of function of def selectively up-regulates Delta113p53 expression to arrest expansion growth of digestive organs in zebrafish. Genes Dev. 2005; 19:2900–11. [PubMed: 16322560]

33. Bertrand JY, et al. Definitive hematopoiesis initiates through a committed erythromyeloid progenitor in the zebrafish embryo. Development. 2007; 134:4147–56. [PubMed: 17959717]

References

1. Belousov VV, et al. Genetically encoded fluorescent indicator for intracellular hydrogen peroxide. Nat Methods. 2006; 3:281–6. [PubMed: 16554833]

2. Bienert GP, Schjoerring JK, Jahn TP. Membrane transport of hydrogen peroxide. Biochim Biophys Acta. 2006; 1758:994–1003. [PubMed: 16566894]

3. Oktyabrsky ON, Smirnova GV. Redox regulation of cellular functions. Biochemistry (Mosc). 2007; 72:132–45. [PubMed: 17367290]

4. Redd MJ, Cooper L, Wood W, Stramer B, Martin P. Wound healing and inflammation: embryos reveal the way to perfect repair. Philos Trans R Soc Lond B Biol Sci. 2004; 359:777–84. [PubMed: 15293805]

5. Renshaw SA, Loynes CA, Elworthy S, Ingham PW, Whyte MK. Modeling inflammation in the zebrafish: how a fish can help us understand lung disease. Exp Lung Res. 2007; 33:549–54. [PubMed: 18075830]

6. Grabher C, et al. Birth and life of tissue macrophages and their migration in embryogenesis and inflammation in medaka. J Leukoc Biol. 2007; 81:263–71. [PubMed: 17046968]

7. Huttenlocher A, Poznansky MC. Reverse leukocyte migration can be attractive or repulsive. Trends Cell Biol. 2008; 18:298–306. [PubMed: 18468440]

8. Maeda H, et al. Fluorescent probes for hydrogen peroxide based on a non-oxidative mechanism. Angew Chem Int Ed Engl. 2004; 43:2389–91. [PubMed: 15114569]

9. Mathias JR, et al. Resolution of inflammation by retrograde chemotaxis of neutrophils in transgenic zebrafish. J Leukoc Biol. 2006; 80:1281–8. [PubMed: 16963624]

10. Hall C, Flores MV, Storm T, Crosier K, Crosier P. The zebrafish lysozyme C promoter drives myeloid-specific expression in transgenic fish. BMC Dev Biol. 2007; 7:42. [PubMed: 17477879]

11. Sen CK, Roy S. Redox signals in wound healing. Biochim Biophys Acta. 2008; 1780:1348–61. [PubMed: 18249195]

12. Bedard K, Krause KH. The NOX family of ROS-generating NADPH oxidases: physiology and pathophysiology. Physiol Rev. 2007; 87:245–313. [PubMed: 17237347]

13. Kawahara T, Quinn MT, Lambeth JD. Molecular evolution of the reactive oxygen-generating NADPH oxidase (Nox/Duox) family of enzymes. BMC Evol Biol. 2007; 7:109. [PubMed: 17612411]

14. Ameziane-El-Hassani R, et al. Dual oxidase-2 has an intrinsic Ca2+-dependent H2O2-generating activity. J Biol Chem. 2005; 280:30046–54. [PubMed: 15972824]

15. ten Freyhaus H, et al. Novel Nox inhibitor VAS2870 attenuates PDGF-dependent smooth muscle cell chemotaxis, but not proliferation. Cardiovasc Res. 2006; 71:331–41. [PubMed: 16545786]

16. Stielow C, et al. Novel Nox inhibitor of oxLDL-induced reactive oxygen species formation in human endothelial cells. Biochem Biophys Res Commun. 2006; 344:200–5. [PubMed: 16603125]

17. Lange S, et al. Platelet-derived growth factor BB stimulates vasculogenesis of embryonic stem cell-derived endothelial cells by calcium-mediated generation of reactive oxygen species. Cardiovasc Res. 2009; 81:159–68. [PubMed: 18806276]

18. Tegtmeier, FD.; Walter, Ulrich (., DE; Schinzel, Reinhard (., DE; Wingler, Kirstin (., DE; Scheurer, Peter (., DE; Schmidt, Harald (., DE; VASOPHARM BIOTECH GMBH (DE). 2005.

19. Donko A, Peterfi Z, Sum A, Leto T, Geiszt M. Dual oxidases. Philos Trans R Soc Lond B Biol Sci. 2005; 360:2301–8. [PubMed: 16321800]

20. Geiszt M, Witta J, Baffi J, Lekstrom K, Leto TL. Dual oxidases represent novel hydrogen peroxide sources supporting mucosal surface host defense. Faseb J. 2003; 17:1502–4. [PubMed: 12824283]

21. Ha EM, Oh CT, Bae YS, Lee WJ. A direct role for dual oxidase in Drosophila gut immunity. Science. 2005; 310:847–50. [PubMed: 16272120]

22. Forteza R, Salathe M, Miot F, Forteza R, Conner GE. Regulated hydrogen peroxide production by Duox in human airway epithelial cells. Am J Respir Cell Mol Biol. 2005; 32:462–9. [PubMed: 15677770]

23. Wesley UV, Bove PF, Hristova M, McCarthy S, van der Vliet A. Airway epithelial cell migration and wound repair by ATP-mediated activation of dual oxidase 1. J Biol Chem. 2007; 282:3213–20. [PubMed: 17135261]

24. Klyubin IV, Kirpichnikova KM, Gamaley IA. Hydrogen peroxide-induced chemotaxis of mouse peritoneal neutrophils. Eur J Cell Biol. 1996; 70:347–51. [PubMed: 8864663]

25. Li W, Liu G, Chou IN, Kagan HM. Hydrogen peroxide-mediated, lysyl oxidase-dependent chemotaxis of vascular smooth muscle cells. J Cell Biochem. 2000; 78:550–7. [PubMed: 10861852]

26. Todorovic SM, et al. Redox modulation of T-type calcium channels in rat peripheral nociceptors. Neuron. 2001; 31:75–85. [PubMed: 11498052]

27. Kwon J, et al. Reversible oxidation and inactivation of the tumor suppressor PTEN in cells stimulated with peptide growth factors. Proc Natl Acad Sci U S A. 2004; 101:16419–24. [PubMed: 15534200]

28. Zhao M, et al. Electrical signals control wound healing through phosphatidylinositol-3-OH kinase-gamma and PTEN. Nature. 2006; 442:457–60. [PubMed: 16871217]

29. Subramanian KK, et al. Tumor suppressor PTEN is a physiologic suppressor of chemoattractant-mediated neutrophil functions. Blood. 2007; 109:4028–37. [PubMed: 17202315]

30. Nishio M, et al. Control of cell polarity and motility by the PtdIns(3,4,5)P3 phosphatase SHIP1. Nat Cell Biol. 2007; 9:36–44. [PubMed: 17173042]
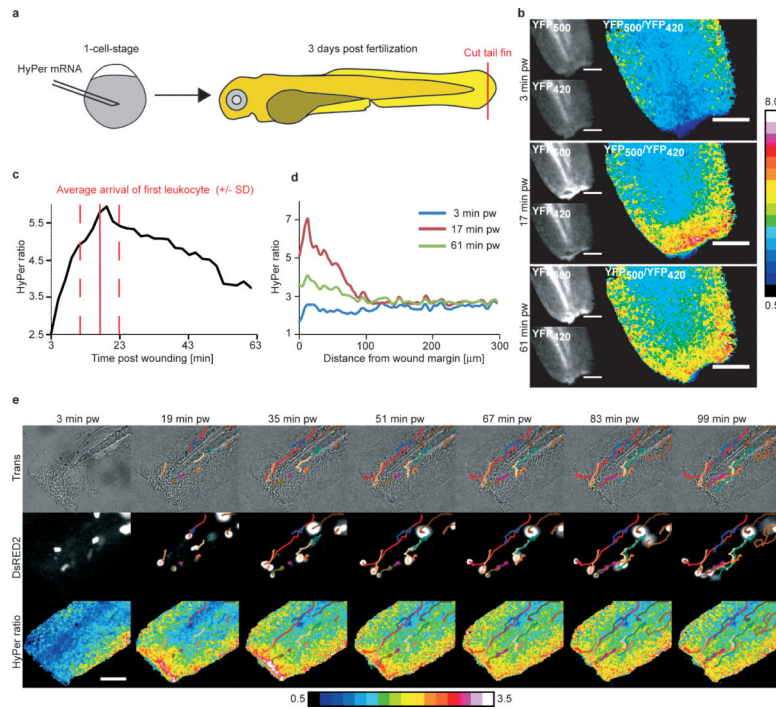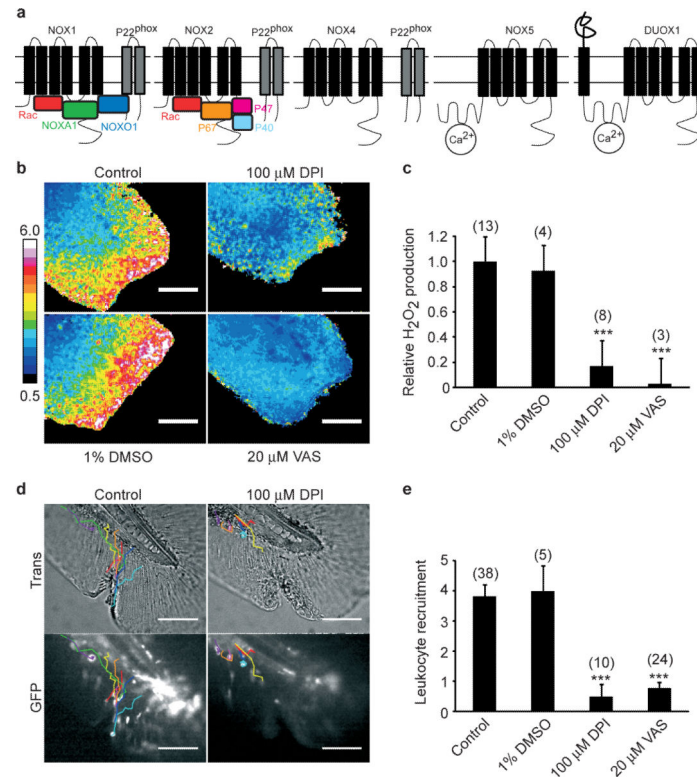
Figure 1.
Wound margin H_2O_2 production in zebrafish larvae. **(a)** Experimental procedure. **(b)** HyPer imaging in an injured zebrafish larva. $[H_2O_2]$ is inferred from the YFP_{500}/YFP_{420} excitation ratio of HyPer. Greyscale scaling is adjusted to improve contrast. **(c)** Temporal $[H_2O_2]$ profile in a ~10–30 μm broad region of interest along the wound margin. Arrival of first leukocyte at wound (solid red line) ± SD (dashed red line). **(d)** $[H_2O_2]$ line profile normal to the wound margin. **(e)** Imaging of leukocyte recruitment and $[H_2O_2]$ in a *lysC::DsRED2*10 fish line. Coloured lines: superimposed leukocyte tracks. Scale bars: 100 μm.

Figure 2.
Nox/Duox activity is required for wound margin H_2O_2 production and leukocyte recruitment. **(a)** Scheme of mammalian NADPH oxidases also found in zebrafish12,13. **(b)** Wound margin $[H_2O_2]$ ± DPI or VAS2870 (VAS), or carrier (1% DMSO) imaged 17 min pw. **(c)** Statistical quantification of wound margin $[H_2O_2]$. **(d)** Injured tail fins of *mpo::GFP*9 larvae ± DPI (42 min pw). Coloured lines: leukocyte tracks derived from the corresponding time-lapse movies. **(e)** Statistical quantification of leukocyte recruitment to wound margin. Error bars: SEM of indicated number of larvae (brackets). *** P < 0.001 (vs. control). Scale bars: 100 μm.
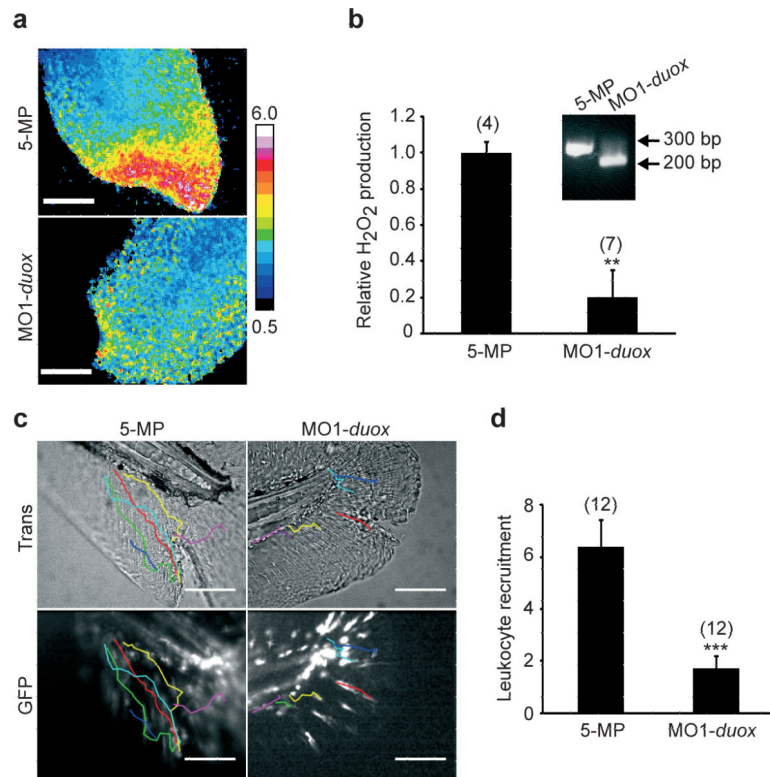
Figure 3.
Duox activity is required for wound margin H_2O_2 production and leukocyte recruitment. **(a)** Wound margin H_2O_2 after morpholino mediated *duox* knockdown (MO1-*duox*) or injection of a corresponding 5-misprime morpholino (5-MP) imaged 17 min pw. Inset: RT-PCR of a *duox* mRNA region flanking the targeted splice site. **(b)** Quantification of wound margin [H_2O_2]. **(c)** Injured tail fins of *mpo::GFP*9 larvae injected with MO1-*duox*, or 5-MP (42 min pw). Coloured lines: leukocyte tracks. **(d)** Quantification of leukocyte recruitment. Error bars: SEM of indicated number of larvae (brackets). ** $P < 0.01$, *** $P < 0.001$ (vs. control). Scale bars: 100 μm.